

A Polymer's Dielectric Normal Modes Depend on Its Film Thickness When Confined between Nonwetting Surfaces

Sangmin Jeon and Steve Granick*

Department of Materials Science and Engineering, University of Illinois, Urbana, Illinois 61801

Received January 3, 2001

ABSTRACT: The dielectric loss peaks of both normal-mode relaxation (fluctuations of the end-to-end dipole vector perpendicular to the confining surfaces) and segmental motion (fluctuations perpendicular to the chain backbone) of *cis*-polyisoprene were measured with special attention paid to contrast between responses of the bulk samples and films ≈ 100 nm thick. The polymers, narrow-distribution samples with number-average molecular weight $M_n = 2600, 6000,$ and $10\,000$ g mol $^{-1}$, were spin-cast onto atomically smooth mica, coated with a second mica sheet, and quenched to temperatures at which the resulting sandwich geometry was kinetically stable although the polymer films dewet these surfaces at equilibrium. The segmental relaxation process was the same for bulk and thin films, but the normal mode (the end-to-end dipole vector relaxation) slowed down, more so as temperature decreased. This loss mode in the capacitance, $C''(f)$, did not for thin films display the expected terminal tail observed in the bulk samples ($C'' \propto f^m$ with $m < 1$ at low frequency f). The power m decreased from 0.9 to 0.5 as temperature was lowered from 260 to 235 K. The inability to quantitatively define the average frequency of this apparently inhomogeneous process led us to analyze the temperature dependence of the frequency at peak of the normal mode. In studies of its temperature dependence, the activation energy of the thin films was found to exceed by 10–20% that for bulk samples and, unlike the bulk state for samples in this range of relatively low molecular weight, to be independent of molecular weight. We interpret these results to indicate that the normal mode not only slowed down but also became more inhomogeneous in this temperature range of 100–30 K above the bulk glass transition temperature, T_g . The contrasting thickness and temperature dependence of the normal-mode and segmental relaxation modes indicates strong breakdown of time–temperature superposition.

Introduction

Remarkable changes in the apparent glass transition in thin polymer films have fueled much recent inquiry into this phenomenon. The classical interpretation of a liquid's mobility and temperature (or pressure), which constitutes the classic, long-standing problem of the glass transition,^{1–3} has been revitalized by the recent theoretical proposition that geometrical length scales, some kind of cooperativity length, appear to enter naturally into the statement of this problem.^{4–9} This has motivated a great deal of experimental work to study shifts of the glass transition when a glass-forming liquid is confined in one or more directions,^{10–12} although this literature and its interpretation are still controversial. A clear-cut answer has been slower to arrive at than was hoped at first.

Upon surveying this complex literature, it is clear that three aspects have proven to be unexpectedly complex. First are the problems of specific boundary effects (a curved pore space or a parallel geometry; attractive or repulsive surface; "hard" solid boundary or "soft" boundary comprised of air or vacuum). In view of these complications when a large portion of one's sample is in intimate contact with the boundary, it has become progressively less clear whether a general answer, independent of the specific boundary, should even be expected. A second problem is that the various measures of the glass transition that seem to give equivalent measures of the glass transition point in the bulk sometimes do not agree when it comes to specifying the point of glass transition in these anisotropic thin films. These methods include, for example, thermal expansivity, translational diffusion, and segmental mobility measured by dielectric or rheological methods.¹² A third

problematical point is that only a limited range of experimental systems can be studied. This problem arises when one is interested to eliminate strong attraction of a sample to its boundary and to study films of such samples at temperatures above the glass transition temperature, T_g . In pursuit of this end, the study of free-standing polymer films, thin strips between air or vacuum, has presented a refreshing simplification that leads to major advances,^{13,14} but their study is limited to situations where the films cannot, owing to high viscosity, bead up to minimize their surface area. This limits their study to temperatures below the glass transition temperature.

Here we introduce a method to study linear, flexible polymers at temperatures tens of degrees or more above T_g , yet under conditions where attraction to the boundary is avoided. The enabling idea was to form the films between nonwetting solids. We find that sandwiches of this kind can be produced that are kinetically stable, although dewetting cannot be eliminated completely. In this situation the normal mode of dielectric relaxation slows down, but the segmental mode does not.

In the study described here, chains of relatively low degree of polymerization were selected so that both local (segmental) and global (normal-mode relaxation of the entire chain) could be measured in the same experiment. Dielectrically active fluctuations of the end-to-end vector were found to slow down and to become progressively more heterogeneous relative to the bulk behavior starting 100 °C above T_g in films as thick as 0.1 μm . The results provide indirect speculative support for the notion of confinement-induced dynamical heterogeneity^{12–14} above T_g .

Experimental Section

Sample and Methods. The glass-forming liquid was *cis*-polyisoprene, whose slowest dielectric dispersion peak on the frequency scale reflects the slowest normal mode of individual molecules because electric dipoles on each repeat unit lie preferentially parallel to the chain backbone. Each repeat unit also possesses a weaker component of the electric dipole normal to the backbone, which makes it possible to measure, in the same experiment, the accompanying dispersion of individual segments.¹⁵ *cis*-Polyisoprene prepared by anionic polymerization has only 81% *cis* content in the head-to-tail configuration and therefore fails to crystallize;¹⁶ it is a model system for studying the glass transition in polymer films.

The *cis*-polyisoprene (PI) samples were purchased from Polymer Sources (Québec) with molecular weights $M_n = 2560$, 6000, and 10 000 g mol⁻¹ and with relatively narrow ratios of weight-average to number-average molecular weight $M_w/M_n = 1.10$, 1.04, and 1.04, respectively. We refer to them below as polymers A, B, and C, respectively. At room temperature, when held in a bottle, all are low-viscosity liquids. They were stored cold under nitrogen and handled with minimum possible exposure to oxygen. In the bulk, the critical molecular weight for entanglement is 10 000 g mol⁻¹,¹⁷ i.e., not less than the molecular weight of these samples. In the bulk state, chains in this range of low molecular weight behave as single Rouse chains whose dielectric response has been studied in great detail.^{15–20} Direct measurement was not made of the bulk glass transition temperature of every sample. (It is known that T_g decreases with decreasing molecular weight owing to greater abundance of chain ends.³) From the dielectric response, the glass transition temperature of the bulk sample of highest molecular weight was determined to be -70 °C.

The technique to measure thin-film dielectric response between sheets of atomically smooth mica at room temperature was described previously.²¹ Here, for the first time, we control temperature over a wide range. This was done by placing the sample within an insulated chamber contained within a Dewar flask through which passed burn-off gas from liquid nitrogen that had been preheated as needed. The temperature uniformity at the sample was ± 0.1 °C. The fractional change of thickness between our lowest measurement temperatures and room temperature (the preparation temperature), owing to thermal expansion, was approximately 4.5%. The experiments and temperature calibration were validated by quantitative agreement, for samples of bulk thickness, with the prior extensive experiments of Adachi.¹⁷ The range of measurement temperatures that we report below was dictated by the need to keep dispersions within the available frequency range: > 1 Hz to avoid distortion from polar surface impurities and $< \sim 3$ MHz by instrumental limitations. The measurements employed a Solartron 1260 gain-phase impedance analyzer connected to a Solartron 1296 dielectric interface.

Briefly, to prepare the samples, the polymer was spin-cast from cyclohexane solution, 1–15 mg mL⁻¹ depending on the desired film thickness, onto a freshly cleaved sheet of muscovite mica that had been cleaved by traditional methods to give atomically smooth, step-free sheets of thickness 1–4 μm and area ≈ 1 cm². After 1 min of spin-coating, a sheet of cleaved mica of this same thickness was placed immediately on top. Control experiments showed the solvent was already evaporated. Capillary forces pulled the second sheet onto the underlying polymer sample, creating a sandwich geometry. Each mica sheet was sputter-coated before use with silver on the backside so that film thickness could be measured between the resulting Fabry–Perot interferometer using traditional surface forces methods²¹ (this was done at room temperature). The silver served the additional function of electrode for the dielectric measurements. About 5 min was required for measurement after about 30 min to equilibrate at each temperature. Dielectric measurements were usually made in the order of ascending temperature, but control experiments verified reversibility.

Dewetting during the long measurement process could not be eliminated completely. Thickness measured by multiple

beam interferometry would usually show uniform thickness over a spot size of 1 mm, but local microscopic dewetting over a spot size of 1 cm was observed in usually 2–3% of the surface by optical microscope, appearing to the eye as bubbles. Many experiments had to be discarded owing to obvious macroscopic dewetting. But the favorable experiments were repeatable, and we have not been able to find a reason why this amount of partial dewetting could explain the results presented below.

We note that an alternative method to prepare thin polymer films between electrode surfaces for dielectric measurements consists of spin-coating the polymer onto one electrode and then sputter-depositing a second electrode onto the polymer thin film.²² The method does not appear to be applicable to the preparation of nonwetting surfaces and presents some uncertainty concerning possible roughness and chemical reactivity, which we sought in the present experiments to avoid.

Analysis of Dielectric Measurements. Elsewhere, it was discussed that when the response to sinusoidal input electric field at frequency f is decomposed into one component in-phase with the field and a second component in-phase with its rate of change, the former (real) component is dominated by the mica buffer sheets between the electrodes and sample, and the latter (loss) component, $C''(f)$, contains an immeasurably small contribution from the mica sheets and reflects only the PI sample.²¹

Specifically, for the measurement of polymer sample between two parallel sheets of mica the complex capacity C^* is given as

$$C^* = \left[\frac{1}{C_m} + \frac{1}{\epsilon_m^* C_{10}} \right]^{-1} = C_m \left[1 + \frac{t_{\text{PI}} \epsilon_m}{t_m \epsilon_m^* C_{10}} \right]^{-1} \cong C_m \left[1 - \frac{t_{\text{PI}} \epsilon_m}{t_m \epsilon_m^* C_{10}} \right] \quad (t_{\text{PI}} \ll t_m) \quad (1)$$

where C_m is the capacitance of the two mica layers, t_m is the total thickness of the two mica layers, ϵ_m is the (f -insensitive) dielectric constant of mica, and t_{PI} is the thickness of the thin, spin-coated PI layer. For this setup, C_m is identical to the capacity measured for the bare mica–mica contact, and t_m and t_{PI} are known from optical interferometry. The quantity ϵ_m can be calculated from C_m (if the electrode area is known) or can be replaced by a literature value. Thus, in principle, it is possible to evaluate ϵ_m^* from experimentally measured values, but the method requires accurate calibration of the empty cell (bare mica capacitance).

In our current experimental setup it was not possible to perform these experiments in an atmosphere sufficiently dry to obtain a sufficiently reliable evaluation of C_m (mica–mica contact). The influence of moisture condensed on the mica surfaces became plain when measurements were performed in nominal mica–mica contact (two cleaved mica sheets placed in contact). The ratio C''/C' was variable between experiments, as discussed elsewhere.²¹ There then resulted a large uncertainty in the capacitance of the two mica layers, C_m , and it was not possible to be confident that C_m measured for mica–mica contact remained the same after spin-coating with PI. Therefore, in the results that follow, the raw data $C''(f)$ will be presented. Because the out-of-phase contribution of the sample cell (mica) to $C''(f)$ was negligible, its frequency dependence is believed to have been the same as for the polyisoprene sample of interest.

Results

Reliability of Measurements. The main difficulties were, first, the matter of signal-to-noise and, second, the need to kinetically prevent dewetting.

Because the dielectric response of thin-film samples was very small, great pains were made to refine and check the electronic circuitry, and numerous repeat experiments were made to verify the data presented below. Various alternative methods of electrical connection and of sample cell design were tried to minimize

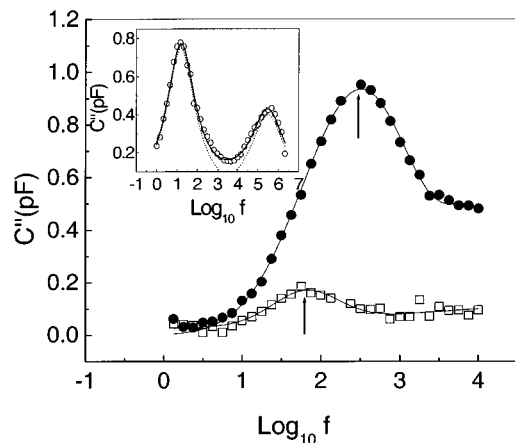


Figure 1. In the main figure, the normal-mode relaxation of dielectric loss, $C''(f)$, plotted against logarithmic frequency, is contrasted for polymer A at -38.5 °C as concerns a sample of bulk thickness (●) and a sample of thickness 100 nm (□). Arrows show the peak frequency inferred from a Gaussian fit to the data. The inset contrasts the normal-mode, f^N , and segmental relaxations, f^S , for a bulk sample of polymer C at -22.5 °C. The dotted lines show a Gaussian fit to the data.

stray capacitance to the utmost extent possible. Various ambient atmospheres, including special drying within a nitrogen-filled glovebox, were tried in order to minimize humidity that otherwise would condense onto the surface and contribute to the low-frequency conductivity. Note that the peaks in Figure 1, $\approx 10^{-13}$ farad (F) at the peak of a dispersion, are 2 orders of magnitude smaller than customary when studying fluids in pores.

In addition, it was a struggle to prevent dewetting. If the samples were allowed to age at room temperature after spin-casting but without adding the second mica sheet, dewetted films with a beautiful spinodal pattern, quantitatively similar to that reported by Xie and co-workers,²³ could be observed by atomic force microscopy (AFM). (Parenthetically, we found it convenient to first sputter-deposit Ag on top to arrest the dewetting process. To be visible in an optical microscope, ≈ 30 min aging at room temperature was usually required, but dewetting was slowed down when the films were confined as a sandwich between two sheets of mica.) Dewetting was more difficult to avoid, the lower the molecular weight of the sample, because the lower viscosity made the sample more prone to dewet at room temperature before it could be quenched. For this reason, the results presented here include more data for polymers B and C than for polymer A.

Although it is an interesting question to consider by what mechanism the films were able to dewet when confined between the two rather rigid solid boundaries of mica, in practice they did. In about 90% of the experiments, after quenching the sample and performing measurements, the sample would return to room temperature with the film decomposed into droplets. Those measurements were discarded. In the successful experiments this was avoided, and spot control experiments verified reversibility. After measurements made at low temperature, the temperature was raised to 25 °C and then lowered back to -40 °C for repeat measurement. Because measurements were reversible, because measurements in the range -40 to 0 °C were stable (time-independent over a period of hours), and because of independent experiments with different time

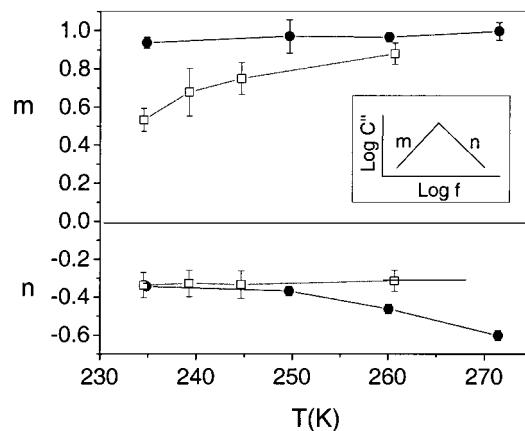


Figure 2. In the main figure, the apparent power $C''(f) \sim f^m$ and $C''(f) \sim f^n$, obtained from a log-log plot of C'' vs f for the normal-mode relaxation peak, is contrasted for thin-film and bulk samples of polymer A as a function of temperature. Here m denotes the power at less than the maximum loss frequency f_{\max}^N and n denotes the power above f_{\max}^N . The inset illustrates the distinction between powers m and n . Error bars are indicated.

and temperature histories were quantitatively reproducible, it was concluded that dewetting processes did not contribute to the results described below.

Normal Mode Relaxations. First we discuss fluctuations of the end-to-end vector of the polymer chain. For polymer A, Figure 1 contrasts this for a bulk sample and a thin-film sample (100 nm thick), both at -38.5 °C (the inset of Figure 1 includes a broader frequency span that shows both normal-mode and segmental relaxation peaks; discussed below). In both the main figure and the inset, dielectric loss is plotted against logarithmic frequency.

There are three main points to notice. First, for the thin-film sample the magnitude of the signal was small; complications resulting from low signal-to-noise were discussed in the previous section. Second, its normal-mode peak was broader than the peak of the bulk sample; this is quantified below. Third, its peak frequency was less than for the bulk sample, indicating a slower relaxation process. It is significant to notice that the measurement temperature was still 30 °C above the bulk T_g of the sample of highest molecular weight.

This and similar data obtained at other temperatures were analyzed. It would have been ideal to be able to analyze according to the Havriliak–Negami equation, classical in the study of glasses,²⁴ but this contains four parameters and the limited signal-to-noise precluded a robust fit. Therefore, as shown in Figure 2, the data were fit to a two-parameter expression, to which it was possible to make robust comparison. To quantify breadth of the peaks they were fitted to power laws, $C''(f) \sim f^m$ and $C''(f) \sim f^n$, where m denotes the power below the maximum loss frequency f_{\max}^N and n denotes the power above f_{\max}^N . Classical "liquid" behavior requires $m = 1$, and for a Rouse chain, it is expected that $n = 1/2$.³

For the bulk samples, Figure 2 illustrates general agreement with these expectations, especially so on the low-frequency side (the parameter m), which agrees perfectly in the present experiments with the classical expectation for a single terminal normal-mode relaxation process. It is true that in other dielectric studies this low-frequency peak does not exactly fit the Rouse model, as has been reviewed by Watanabe,²⁰ but the

point does not seem to be essential when one considers that the results presented in this paper, and discussed below, are corroborated by a parallel series of experiments on a second system, poly(propylene glycol) containing added LiClO_4 .²⁵

Figure 2 shows that for the thin-film sample deviations from $m = 1$ were observed at every temperature, increasingly so as the temperature was lowered. With decreasing temperature, the value of m decreased from 1 to 0.5. This we will take to indicate "heterogeneity", though whether it stems from a distribution of relaxation processes, or an intrinsically complex relaxation process, cannot be determined from the data at hand. There is precedent for observing heterogeneity for local-mode relaxation, the so-called α -process.¹⁹ The new point was to observe these deviations so far above T_g and for a process that involved collective motions of many segments—not a segmental process, as in the classical α -process, but in fluctuations of the end-to-end dipole vector. Note that the data in this comparison refer to a single film thickness, ≈ 100 nm; the experiments were exceptionally difficult owing to the need for high signal-to-noise in order to resolve the power laws m and n with confidence.

While it is true that the temperature dependence of the peak of a distribution that is changing shape may not be easily interpreted, the average frequency of this asymmetric mode could not be calculated with confidence from the data. Ideally, one would integrate the distribution represented by the complex peak shape to determine the mean frequency, but we found that the signal-to-noise of the data did not permit this to be performed with sufficient confidence to warrant further analysis. Therefore, as a practical matter, to analyze the temperature dependence of these modes, we proceeded to compare their peak frequencies. In Figure 3 (top panel), the peak frequencies are plotted logarithmically against inverse temperature, and responses of the bulk and thin-film samples are contrasted.

For thin films, one observes that all three samples, polymers A, B, and C, appeared to follow linear relations over this temperature range, which may be interpreted as a constant activation energy for the process measured. This is interesting and unexpected because it is known³ that in the bulk state relatively short polymer chains display different apparent activation energies of normal-mode relaxation owing to the different relative influences of chain ends to the total volume. Indeed, this expected difference is confirmed for our bulk samples by the data shown in Figure 3.

The inset of Figure 3 (top panel) shows the deduced apparent activation energies. For the bulk samples the activation energy increased as expected with increasing molecular weight. If the temperature window is extended to a larger range, it is no longer described well by an Arrhenius relationship and displays that the expected Vogel–Fulcher behavior if the temperature window is extended.^{3,15,16} In stark contrast, for the present thin films the apparent activation energy was the same regardless of molecular weight (90 kJ mol^{-1}). This number in every case exceeds the number that we measured for the bulk samples (64 , 76 , and 79 kJ mol^{-1} for polymers A, B, and C, respectively).

Figure 3 (bottom panel) shows the peak frequency plotted against linear temperature. This representation of the same data as in the top panel shows clearly that, at a given temperature, the peak frequency in the thin

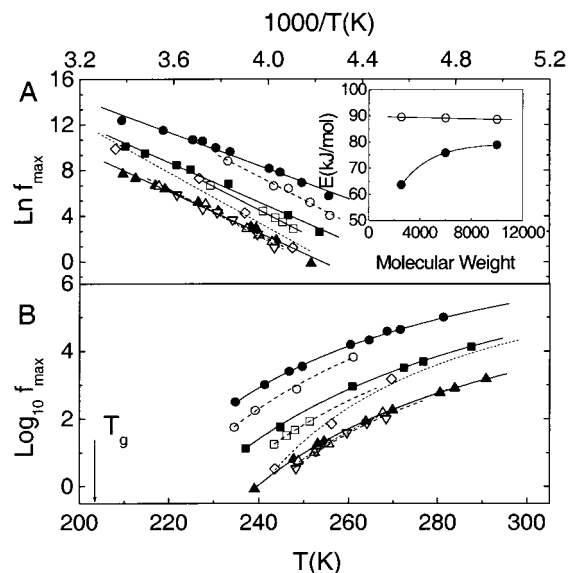


Figure 3. Peak frequency of normal-mode relaxation, f_{max}^N , evaluated by Gaussian fit to the data, is plotted against temperature in two ways. Top panel: natural logarithmic f_{max}^N is plotted against inverse absolute temperature, showing that the apparent Arrhenius activation energy, which depends on molecular weight for bulk samples, was shifted to be nearly the same for these same samples in thin films. Inset of top panel shows the apparent activation energy plotted against molecular weight of the sample polymer. Symbols: polymer A (●, bulk; ○, 101 nm), polymer B (■, bulk; □, 106 nm; ◇, 19 nm), polymer C (▲, bulk; △, 157 nm; ▽, 57 nm). Bottom panel: the ratio of common logarithmic f_{max}^N in the bulk, to common logarithmic f_{max}^N in the thin film at a given temperature, which quantifies retardation in the thin film relative to the bulk, is plotted against absolute temperature. Symbols are same as for top panel. On the abscissa, the bulk T_g is indicated for comparison.

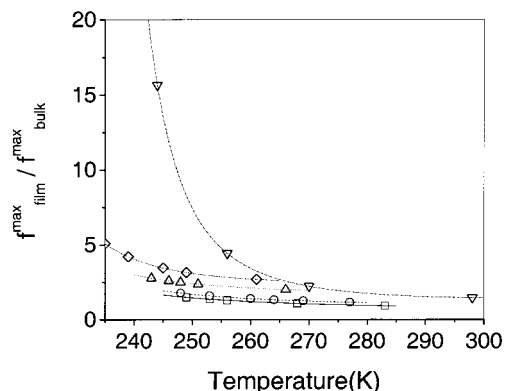


Figure 4. Ratio of peak normal-mode frequency, in the bulk and in thin films, is plotted against absolute temperature for polymer A, thickness 101 nm (◇), and polymer B, thickness 106 nm (△), polymer B, thickness 19 nm (▽), polymer C, thickness 157 nm (□), polymer C, thickness 57 nm (○). For reference, bulk T_g of polymer C was measured to be 203 K.

films was lower than for the bulk samples. The discrepancy was larger, the lower the temperature, yet even the lowest temperatures examined were still 30 deg above the glass transition temperature of polymer C.

Thickness dependence is summarized in Figure 4, where the ratio of the peak relaxation frequency, in the bulk and in the thin films, is plotted against temperature. Peak relaxation frequencies of bulk and thin film are fitted with VFT equations as shown in Figure 2B, and their ratios are calculated. It is evident that

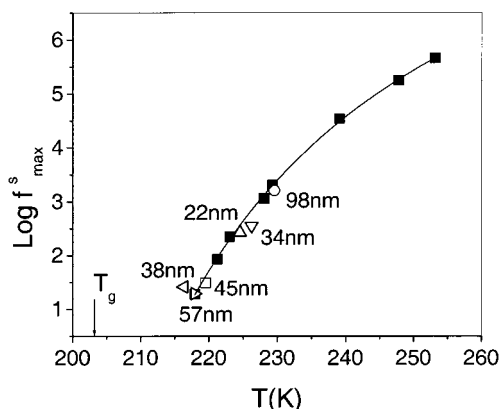


Figure 5. Peak frequency of segmental relaxation, f_{\max}^s , evaluated by a Gaussian fit to the data, is plotted against absolute temperature when evaluated at various film thicknesses as shown by the indicated numbers in units of nanometers. Solid symbols (■) denote samples of bulk thickness. The data concern polymer C. The line through the bulk data agrees quantitatively with measurements of Adachi.¹⁵ The bulk T_g is also shown.

retardation began at higher temperatures, the thinner the film and the lower its molecular weight.

Segmental Mode Relaxations. No confinement-induced shifts were observed as concerns the dielectric dispersion of individual segments. The peak segmental dispersion frequency is plotted against temperature in Figure 5. These data concern polymer C because, for this sample of largest molecular weight, the cleanest separation between local and global relaxation modes could be made (an example is shown in the inset of Figure 1). It is obvious that the temperature dependence of segmental relaxation was unaffected by confinement. In addition (also in contrast to the behavior of the normal mode), the shape of the relaxation peak was unaffected, within the experimental uncertainty.

Discussion and Outlook

This paper raises three main puzzles. The first is to understand why bulk behavior was not observed for these relatively thick films, ≈ 100 nm thick. The second is to understand the different temperature dependence of normal-mode and segmental relaxation dynamics. The third is to understand the loss, in the thin films, of the molecular weight dependence of activation energy that is observed in the bulk samples.

Concerning the first point, it is amazing to observe dependence on film thickness for samples that were so thick relative to the molecular dimension. The end-to-end distances can be estimated as $R_{ETE} \approx 3$ and 6 nm for polymers A and C, respectively; therefore, the total thickness at 100 nm was $\approx 30R_{ETE}$ and $15R_{ETE}$ for polymers A and C, respectively.

Concerning the second point, in mainstream theories of polymer dynamics there is supposed to be no difference between the temperature dependence of normal-mode and segmental relaxations; both are proportional to the monomeric friction coefficient.^{3,26} The relaxation rate of the chain is separated into the product of the monomeric friction coefficient and geometrical factors that describe the chain itself, and the differences according to the degree of polymerization (N) depend on factors of N . The success of this interpretation is the basis of time-temperature superposition.^{3,26} The data presented above can be interpreted as showing signifi-

cant breakdown of time-temperature superposition in these thin films.

While there is some precedent for discrepancy when a bulk sample approaches T_g ,^{27,28} the new points here are 3-fold. First, for bulk samples those effects are observed only in much closer proximity to T_g , closer to T_g by an order of magnitude of temperature in kelvin.^{3,27,28} We emphasize that all of these experiments concern temperature at least 30 K above the bulk T_g . Second, we find the paradoxical result that in the thin films the magnitude of discrepancy was largest for the chains of the *smallest* molecular weight. This is interesting because it has often been supposed that decoupling of long-range and segmental motions would scale with the overall size of a molecule.^{12,13} In this view, confinement would affect most the chains of largest size (least thickness in units of the molecular dimension). This line of logic predicts that discrepancies would increase, the larger the molecular weight, which goes in the direction opposite to the data.

We have given much thought to possible mechanisms by which it might be possible to explain these findings trivially. First, concerns have often been expressed, regarding the case of much higher molecular weight chains than in the present study, that anomalous behavior related to the glass transition in thin polymer films might be introduced by orientation induced by spin-coating. In those samples it might not be possible to anneal spin-induced orientation completely, but this would not be reasonable to argue here. The anomalies reported here were largest for the samples of lowest molecular weight, whose relaxation time was the most rapid, and furthermore the sample preparation times far exceeded the longest relaxation times ($\approx 1/f_{\max}$), measured directly in these experiments. Therefore, the chain configurations in these thin-film samples appear to have been equilibrated. Second, it is not reasonable to explain these findings by supposing that the sample became partitioned into two populations, one with the same properties as a bulk sample and a second with surface-modified properties, as has been done for fluids confined within curved pores;^{18,29} the thickness of a surface-bound layer, on the order of the molecular dimension (end-to-end distance $R_{ETE} \approx 3$ and 6 nm for polymers A and C, respectively), was too much less than the total thickness. Therefore, the preponderant contribution to the measured responses should come from chains in the interior of the confined geometry. Third, it does not seem reasonable to dismiss these results as a trivial outcome of dewetting. While it is true that some small amount of dewetting was always present, metastable thin films could be produced, and reversibility of these measurements was confirmed (as discussed in the Experimental Section).

Therefore, all things considered, we take the three puzzles summarized at the beginning of this section as legitimate challenges for theoretical understanding. This study differs from most studies in this area in that the confinement was symmetric and without strong attraction to the walls. In this respect it resembles the study of free-standing films,¹³ but unlike that case the approach to study dielectric responses after confinement between dewetting solid surfaces makes it possible to study normal-mode responses significantly above the bulk glass transition temperature. Whether the rigidity of the walls might influence chain relaxation times owing to mechanical interaction with viscoelastic eigen-

modes³⁰ is an interesting recent suggestion. Finally, it is worth commenting on the intriguing observation that these experiments find, seemingly paradoxically, that the largest deviations from bulk response were observed for the chains of smallest molecular weight. It happens that the unperturbed molecular dimension of those chains, $R_{\text{ETE}} \approx 3$ nm, is close to the length scale of dynamical heterogeneity, about 3 nm, that emerges from independent experiments on other "glassy" systems in the bulk.^{4,5} Whether the common length scale is coincidental, or fundamental, has not been determined. Indeed, it remains an open question whether these confinement-induced effects have a fundamental relation to the glass transition problem or perhaps stem for other reasons from geometrical confinement.

Recently, we have measured qualitatively similar slowing down of the normal mode, but not the segmental mode, when poly(propylene glycol) with added LiClO₄ salt (a conducting polymer system) is confined between mica sheets to also form a sandwich-shaped thin film.³¹ To observe the same in this second system of flexible polymer chains suggests that the phenomenon is not system-specific.

Acknowledgment. We are indebted to Y.-K. Cho, H. Watanabe, and K. S. Schweizer for discussions and to Y.-K. Cho for initiating this experiment. The work was supported by the Petroleum Research Fund, administered by the American Chemical Society, and by the U.S. Department of Energy, Division of Materials Science, under Award DEFG02-91ER45439 to the Frederick Seitz Materials Research Laboratory at the University of Illinois at Urbana-Champaign.

References and Notes

- (1) Adam, G.; Gibbs, J. H. *J. Chem. Phys.* **1965**, *43*, 139.
- (2) Goldstein, M. *J. Chem. Phys.* **1969**, *51*, 3728.
- (3) Ferry, J. D. *Viscoelastic Properties of Polymers*, 3rd ed.; Wiley: New York, 1980.
- (4) Cicerone, M. T.; Blackburn, F. R.; Ediger, M. D. *J. Chem. Phys.* **1995**, *102*, 471.
- (5) Tracht, U.; Wilhelm, M.; Heuer, A.; Feng, H.; Schmidt-Rohr, K.; Spiess, H. W. *Phys. Rev. Lett.* **1998**, *81*, 2727.
- (6) Onuki, A.; Yamamoto, R. *J. Non-Cryst. Solids* **1998**, *235*, 34.
- (7) Bennemann, C.; Donati, C.; Bashnagel, J.; Glotzer, S. C. *Nature* **1999**, *399*, 246.
- (8) Wang, C.; Ediger, M. *J. Chem. Phys.* **2000**, *112*, 6933.
- (9) Hempel, E.; Hempel, G.; Hensel, A.; Schick, C.; Donth, E. *J. Phys. Chem. B* **2000**, *104*, 2460.
- (10) McKenna, G.; et al. *J. Non-Cryst. Solids* **1991**, *131*, 528.
- (11) Keddie, J. L.; Jones, R. A. L.; Cory, R. A. *Europhys. Lett.* **1994**, *27*, 59.
- (12) For references to a large literature, see: Fryer, D. S.; Nealey, P. F.; de Pablo, J. J. *Macromolecules* **2000**, *33*, 6439. Ge, S.; et al. *Phys. Rev. Lett.* **2000**, *85*, 2340. Park, J.; McKenna, G. *Phys. Rev. B* **2000**, *61*, 6667. Forrest, J.; Mattsson, J. *Phys. Rev. E* **2000**, *61*, R53.
- (13) Forrest, J.; Dalnoki-Veress, K.; Dutcher, J. *Phys. Rev. E* **1997**, *56*, 5705.
- (14) Dalnoki-Veress, K.; Forrest, J. A.; de Gennes, P.-G.; Dutcher, J. R. *J. Phys. IV* **2000**, *10*, 221.
- (15) Adachi, K.; Kotaka, T. *Macromolecules* **1985**, *18*, 466.
- (16) Boese, D.; Kremer, F. *Macromolecules* **1990**, *23*, 829.
- (17) Adachi, K.; Kotaka, T. *Prog. Polym. Sci.* **1993**, *18*, 585.
- (18) Boese, D.; Kremer, F. *Macromolecules* **1990**, *23*, 829.
- (19) Boese, D.; Kremer, F.; Fetters, L. *Macromolecules* **1990**, *23*, 1826.
- (20) Watanabe, H. *Macromol. Rapid Commun.* **2001**, *22*, 127.
- (21) Cho, Y.-K.; Watanabe, H.; Granick, S. J. *Chem. Phys.* **1999**, *110*, 9688.
- (22) Fukao, F.; Miyamoto, Y. *Europhys. Lett.* **1999**, *46*, 649.
- (23) Xie, R.; et al. *Phys. Rev. Lett.* **1998**, *81*, 1251.
- (24) Havriliak, S.; Negami, S. *J. Polym. Sci., Part C* **1996**, *14*, 99.
- (25) Kojio, K.; Jeon, S.; Granick, S., submitted for publication.
- (26) Doi, M.; Edward, S. *The Theory of Polymer Dynamics*; Clarendon: Oxford, 1986.
- (27) Schonhals, A. *Macromolecules* **1993**, *26*, 1309.
- (28) Plazek, D.; et al. *J. Chem. Phys.* **1993**, *98*, 6488.
- (29) Rizos, A.; Fytas, G.; Semenov, A. *J. Chem. Phys.* **1995**, *102*, 6931.
- (30) Herminghaus, S.; Jacobs, K.; Seemann, R. *Eur. Phys. J. E* **2001**, *5*, 531.
- (31) Kojio, K.; Jeon, S.; Granick, S., submitted for publication.

MA010015X